Asian Journal of Chemistry; Vol. 33, No. 12 (2021), 2871-2884

ASIAN JOURNAL OF CHEMISTRY

https://doi.org/10.14233/ajchem.2021.23392

REVIEW

Recent Advantages and Applications of Various Biosynthesized Greener Silver Nanoparticles

K. CHINNAIAH[1], T. THIVASHANTHI[1,*], ASADOLLAH ASADI[2], A. MUTHUVEL[3], KARTHIK KANNAN[4], M. GOHULKUMAR[5], VIVEK MAIK[6] and K. GURUSHANKAR[1,7,*]

[1]Department of Physics, School of Advanced Sciences, Kalasalingam Academy of Research and Education, Krishnankoil, Virudhunagar-626126, India
[2]Department of Biology, Faculty of Science, University of Mohaghegh Ardabili, Ardabil, Iran
[3]PG and Research Department of Physics, T.B.M.L. College (Affiliated to Bharathidasan University, Tiruchirappalli), Poaryar-609307, India
[4]School of Advanced Materials Science and Engineering, Kumoh National Institute of Technology (KIT), 61 Daehak-ro, Gum-si, Gyeongbuk, 39177, Republic of Korea
[5]P.G. and Research Department of Physics, Vivekanandha College of Arts and Sciences for Women (Autonomous), Elayampalayam-637205, India
[6]Department of Electronics & Communication Engineering, SRM Institute of Science and Technology, Kattankulathur Campus, SRM Nagar, Kattankulathur-603203, India
[7]Laboratory of Computational Modeling of Drugs, Higher Medical and Biological School, South Ural State University, Chelyabinsk-454080, Russia

*Corresponding author: E-mail: gurushankar01051987@gmail.com

Received: 30 June 2021; *Accepted*: 23 August 2021; *Published online*: 6 December 2021; AJC-20577

Green synthesis is an effective method for the synthesis of metal and metal oxide nanoparticles. The strong affinity nature of phytochemicals has been effectively utilized as a source of non-toxic nanoparticle production. The optimized pH, concentration, temperature, reaction time needed for non-aggregated and stable biosynthesis silver nanoparticles. The surface modifications of silver nanoparticles over the functionalization of natural compounds are generated unbelievable new thoughts on its properties. Biomolecules in plant extract redirect different safe and size on designed material, which cater as key instruments for harvesting the UV-region. The bio-interaction of structural integrity silver nanomaterial's are promoted the reactive oxygen species in the wound, redox peak potential on cyclic voltammetry, spectral alteration at surface plasmon resonance (SPR) effect and redox reaction on the degradation of organic dyes. In this review, the utilization of different biological compounds and their role of mechanism in the evergreen latest application of colorimetric sensing, electrochemical analysis, wound healing and catalyst areas is discussed.

Keywords: Green synthesis, Natural compound functionalization, Silver, Surface plasmon effect, Redox reaction.

INTRODUCTION

The rapid evolution of material sciences and nanoparticles is considered as the latest promising platform to expanded applications as today and tomorrow [1]. The ability to tune the size, shape, structure and composition helps to reach that goal with a wide range of benefits [2]. Enhancing the optical properties of surface plasmon resonance (SPR) and electronic properties of high extinction coefficient in visible region noble metal nanoparticles have much consideration in the field of catalysis, sensor and therapy [3]. Recent research attention has been developed to searching for metallic nanoparticles, which are well known for exploring the properties of optical, electrical and magnetic. These attractive properties offered technological advancement in many areas such as chemistry, biology, medicine, agriculture and so on [4].

The physical effect of SPR provides the strong electromagnetic confinement around the surface of the nanostructure material; this hotspot leads to the tumor-killing effect, photocatalytic activity, photonic devices, solar cells, light emitting diode, laser diodes and biosensors [5].

Among the noble metal, silver nanoparticles are the best choice for surface plasmon resonance production material as well as eco-friendly and cost-effective, high abundance and modest bioavailability in nature. Therefore it's gained much focus in research [6]. To compare than counterparts, silver nanomaterial's having a unique surface, morphological properties and nanosized behaviour, which are widely used in day to day life in many industries like photography, jewelers, laptops, refrigerator, dietary supplements, clothing, children's toys, food packing and coins [7]. Besides, due to the antimicrobial nature, it applies to health care and hygienic applications such as toothbrushes, cosmetics, plasters and dental alloys. Biosynthesized silver nanoparticles have been proven as one of the best promising metallic nanoparticles for biological applications of various fields such as medicine for antimicrobial and anticancer activities, organic catalyst and can be utilized as medical devices like catheters, clothing and vascular grafts [8]. Metallic silver nanoparticles generated in various natural products from the ariel parts of the plant extract, marine organisms like bacteria, fungus, algae [9]. Biogenic AgNPs is one of the good media for the growth of pathogenic microorganism and using an organic molecule can modify the metallic structure and chemical properties. Hence, it is possible to penetrate the body to interact with biological barriers, tissue and cells [10]. Since necessities still now develop most common engineered nanomaterial with various advantages. Well defined silver nanoparticles can be produced either through chemically or physically. However chemical reduction method generally needed strong reducing agents such as sodium borohydride, hydrazine, *etc*. [11]. These issues can be replaced by natural bio templates, which are non-toxic, clean and green routes.

Green synthesis has emerged a suitable technique in the usage of biological entities and acts as reducing, stabilizing agents in the biomedical field with multiple advances such as small size, ability to interact at a sub-atomic level, easily scaled up and inexpensive method [12]. The synthesis of nanoparticles from plant extract having several advances compare than physical, simple chemical methods, easy availability, low cost, safe to handle, eco-friendly and wide variety of metabolism, the reducing and stability of biogenic-AgNPs got from the natural compounds are presenting on the plant such as proteins, carbohydrates, steroids, alkaloids, *etc*.

The noxious chemical hazards enter into the environmental progressively increases day by day. Metal ions are the most toxic chemical hazards even in the low concentration make the ultimate damaging effect in human life. The major health hazards like acrodynia, minamata, hunter Russell syndrome are created by containing Hg^{2+} ions in the ecosystem, Mn(II) excess exposure causes the neurological disorder and learning disability in children [13], Cd exhibit the symptoms of shorting of life span, hypertension, gross abnormalities [14] over intake of Cu^{2+} resulting in increased blood pressure, Alzheimer disease, amyotrophic lateral sclerosis, Menkes and Wilson disease, as in the case of As(III) causes skin lesions, keratosis, lung, bladder cancer. Therefore, the ability to detect trace metal ion below the designed safety level is an important phenomenon for human health and aqueous environment [15]. In this regard, a number of traditional methods are available for the detection of metal ions, *e.g*. mass spectroscopy, atomic absorption spectroscopy and fluorescent spectroscopy. But these techniques have limitation with need of high expansive and sophisticated facilities instruments still now. UV-visible spectroscopy used as a preliminary identification technique and play a major role in monitoring the degradation and colorimetric detection process. Colorimetric nanosensor approaches popularly crown due to their sensing response through the naked eye [13,16]. Most of them work based on plasmonic nanoparticle aggregation. Silver nanoparticles have considered as good colorimetric material due to their strong SPR band extinction. From the traditional method of environmental and biological analysis, electrochemical techniques are one of the unique and alternative technologies for the detection of ions. Since, they provide concern outputs like accurate, atomization and high accuracy. Sensing purposes the usage of silver gained attention in electrochemical analysis particularly nowadays [17]. The functionalization of AgNPs prevention the surface of nanoparticles oxidation, which enhances capability, stability and applicability and hence this modification can design the new material with different properties [18].

Catalytic degradation is well and good employment for the treatment of wastewater technology due to dispersive nature in the water and cleaning process [19]. Organic dyes are a major part of the chemical compound which is used in degradation with metal nanoparticles one of the best methods of choice nowadays. So many dyes have been limited with several disadvantages for usage. Rhodamine B synthetic water-soluble xanthenes organic dye causes symptoms of chest pain, tearing of eyes, cough, burning of the throat [20], the azo dyes like methyl orange make a toxic effect in oral ingestion, eye irritation, aquatic flora and fauna [21]. Methylene blue is a heterocyclic aromatic compound that mainly contributed to water pollution [19]. Good colloidal stability of AgNPs used as well catalyst for promoting the reduction reaction, which is facilitated by the rich electron in plant extract [22]. The wound healing process is fascinating in the field of tissue engineering and regeneration [23] and normally having three phase inflammation, tissue formation and remodeling. Although, significant biomaterials are need to develop with anti-inflammatory and antimicrobial nature in the wound healing regime. AgNPs loaded wound dressing have much interest due to the antimicrobial activity. The role of Ag^{+} ions releasing in AgNPs still is uncertain it will produce multiple mechanisms of oxidative stress, interactions of enzymes and proteins, inhibition of DNA replication, inducing apoptosis, suppression of anti-apoptosis gene are contributes the anticancer activities [24]. In this review, we are addressed biological compound incorporated AgNPs based on recent research works in various fields of some trending applications nowadays.

Colorimetric analysis of AgNPs: The metal ion sensor is one of the challenging and significant in the field of biosciences and it plays a vital role in the detection of environmental samples [14]. Most of the heavy metal ions are produced from industrial workplaces such as electroplating, chrome plating, wood preservation, alloying, batteries, fixing pigments,

water cooling towers and so on. While these metal ions creating the pollution in of air, water, soil and their permissible limit of metal ions intake on human body gained the good impact on different physiological system when entering through drinking of water, breathing and food items, *etc*. [3,25]. Many health issues including liver damage, cancer risk, cellular toxicity, gastrointestinal disturbance and kidney damage are produced by an overdose of heavy metals due to accumulation in human parts resulted in long term toxicity [26]. Hence, we needed a simple and fast detection method to find out the essential trace metals. Optical sensors are unique due to the cost-effective, rapidity, high sensitivity and SPR properties of metallic nanoparticles. Particularly, silver-based colorimetric sensors are now getting great attention because of their distinctive optical properties, which is used to detection of toxic ions even by the naked eye [27]. Biosynthetic method of AgNPs using aerial parts of the plant as stabilizing as well as reducing agents required longer reaction time employed as most preferable for ions detection [28]. Although, here we examine few studies and their discussion of green synthesized AgNPs based sensors using plant extract employed as a colorimetric sensor for detection of toxic heavy metal ions through sensitivity and selectivity with other heavy metal ions using without costly instruments.

Das *et al.* [29] synthesized *Hibiscus mutabilis* (HM) mediated AgNPs for investigation on colorimetric recognition of Hg^{2+} ions detection. The synthesized AgNPs found to be in a round safe smooth surface with a size of 8 nm, which is illustrated in SEM images and dynamic light scattering. The carboxylic acid, -OH, -C=O functional group in extract stimulates the HMNPs synthesis and it could be used to100% metallic nanoparticles production. This high degree of crystallinity could be making face center cubic crystal structure (FCC) in AgNPs formation due to the self-stabilizing power of HM extract. The HMNPs formation mechanism justification from the diminishment of –OH and –CO band in FTIR spectroscopy and their encapsulation conformed from two fitted peaks in Ag3*d*-spectra in XPS arrangement such as 368.09 eV assigned to Ag^0 for $3d_{5/2}$ and 373.8 eV assigned to Ag^+ for $3d_{3/2}$ shows in Fig. 1. They reported that amalgam formation of Ag(Hg) causes the maximum absorption of HMNPs that appeared at 432 nm with a blue shift in UV-Vis spectra due to the single-particle scattering probability during the reduction process of Hg^{2+} to Hg^0 [30]. The redox reaction between Ag^0 and Hg^{2+} makes a disintegration of HMNPs into smaller particles, it will reflect the colour changes of the solution when the addition of Hg^{2+}. This is indicated from SEM images of HMPS plus Hg^{2+} conjugates and the existence of some large particles reveals that HMNPs surface absorbed the Hg^0 as aggregated particles [31,32]. Hence, they conclude that amalgam Ag(Hg) formation and mechanistic study proceeds lower detection limit (30 ppm) of Hg^{2+} sensing through the oxidation of Ag^0 by Hg^{2+} [33].

Samari *et al.* [34] used mango leaf extract for the synthesis of AgNPs. The oxidation of AgNPs to Ag^+ by Hg^{2+} originates from the smaller particles disintegration of AgNPs and agency of Hg^{2+} reduction to elemental Hg and it reflected an appreciable blue shift on absorption maximum with a detection limit

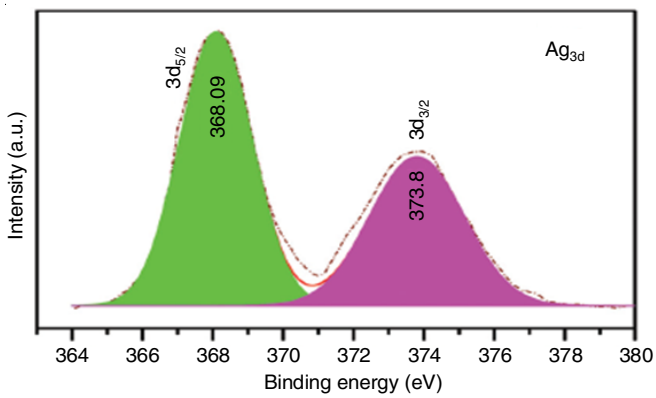

Fig. 1. XPS arrangement of Ag_{3d} adopted from Das *et al.* [29]

of 0.5 ppm. The polyphenols compound such as mangiferin exhibits their double bond conjugated structure *via* π-π* transition show up at 262 nm in UV-vis spectra due to the absorbance of benzyl system. The low stabilizing, reducing the ability of leaf extract on high temperature (80º, 60 ºC) gives a decreased and broad SPR. The more number of biomolecules are producing a large amount of AgNPs with instability because of immediate particle precipitations. The secondary reduction of silver ions leads to the larger size silver nanoparticles on a higher amount of Ag^+ concentration and formation suppressed on acidic conditions with the result not showing SPR peak. The crystalline band of the organic compound in extract found at 32.1º, which is predicted from XRD analysis while this result could be used to the conformation of nanoparticle growth in (111) plane [35]. Vellaichamya & Periakaruppan [36] synthesized *Ceiba pentandra* leaf mediated AgNCs for the demonstration on sensing mechanism of industrial effluents bivalent copper ion as a target molecule in the different water sample. Here, the XRD pattern of AgNPs shows with diminutive intensity, which displays the presence of an excess of $AgNO_3$ concentration while these results replicate morphology of formed nanoparticles in different shapes with size (Fig. 2). The complete formation of AgNPs with *Ceiba pentandra* leaf extract completed within 60 min after that did not indicate further increment on SPR peak; hence it has the possibility to the production of number nanoparticles from increased reaction time. High stability of AgNCs caused by chemisorb on Ag ligand with phenol, carboxyl, amino groups in one end and other end binds with Cu^{2+} ions through the leaching of AgNCs. Hence, Ag^+ and Cu^{2+} are reduced to Cu during the oxidization of AgNCs and their reduction between Ag^0 and Cu^{2+} making colour changes in spectral lines. Non aggregated, size and safe controlled AgNCs due to the phytoconstitution shows increased magnitude of three orders in the detection limit [37]. For instance, Jabariyan & Zanjanchi [38] perform modified graph juice mediated AgNPs for the detection of Cd^{2+} ions over the method of colorimetric sensing. The lone pair of electrons contains a hydroxyl group of riboflavin, ascorbic acid and phenolic compounds which are well bound with Cd^{2+} and their cross linking making a complex formation. This result might be direct the interparticle distance in neighboring nanoparticles and its mirror discloses on SPR peak shifting from 410 to 580 nm. The ratio of extinction coefficient on

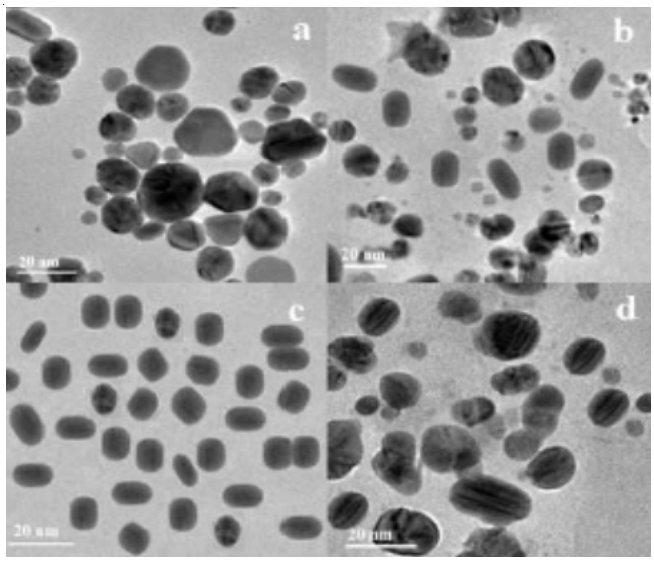

Fig. 2. HR-TEM images of AgNPs synthesized from CPLE with different concentration of $AgNO_3$ adopted from Vellaichamy & Periakaruppan [36]

developed AgNPs is more appropriate for Cd^{2+} detection with a detection limit of 4.95 µmL/L. The high absorption sharp peak and the relative amount of AgNPs can appear on pH 11 at 70 ºC only and its lower pH, temperatures are displayed lock of AgNPs formation shows in Fig. 3. Similarly, Kumar *et al.* [13] developed B-AgNPs bhilwa nuts for the detection of Mn (II) ions in pond water. The population of B-AgNPs increased at the maximum at 80 ºC and SPR beak increased from the pH range of 6 to 9 after that SPR peak intensity decreased slowly when increasing of heating temperature and pH due to the destabilization of B-AgNPs while their whole formation fulfills within 8 min. The average size of prepared nanoparticles is 19 nm and it displayed long term stability even after six months any without aggregation. The oxygen present in the polyphenolic compound of bhilwa nut extract bonded with Mn(II) ions. This metal-ligand interaction induced

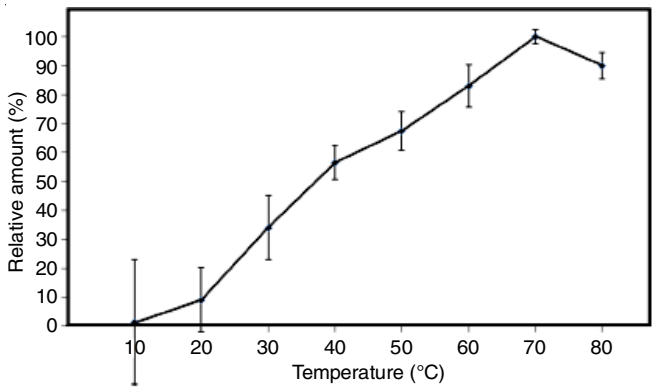

Fig. 3. AgNPs formation related to temperature adopted from Jabariyan & Zanjanchi [38]

redshift on the SPR peak from 404 nm to 432 nm through chemisorb on the functional of bhilwa nuts extract with the surface of AgNPs. While they tell us, a mixture of metal actions do not create any spectral alteration in B-AgNPs as well as the function of Mn(II) attributed to visual colour changes on photographic images with the lowest detection limit of 0.001 ppm by naked eyes.

Ihsan *et al.* [6] investigated Zn^{2+} ions colorimetric sensing performance of AgNPs using *amomum subalatum*. The polyphenols in extract and synthesized AgNPs on room temperature are shows absorption narrow peak at 280, 451 nm, respectively. They are increasing the reaction temperature to needed on minimizing reaction time, which could be reflected as a result of disappeared polyphenols absorption peaks. This result confirmed that plant molecules completely utilized on Ag^{+} ions reduction at the same time remained that all the plant materials are not capable of reducing and stabilizing ability at room temperature. The UV spectra show an increasing concentration of AgNPs depicts a blue shift from 435 to 425 nm and plant extract exhibits redshift from 425 to 450 nm shows in Fig. 4a by the addition of leaf extract ranging from 1.5 mL to 4 mL. This displayed that the equal amount of concentration entirely

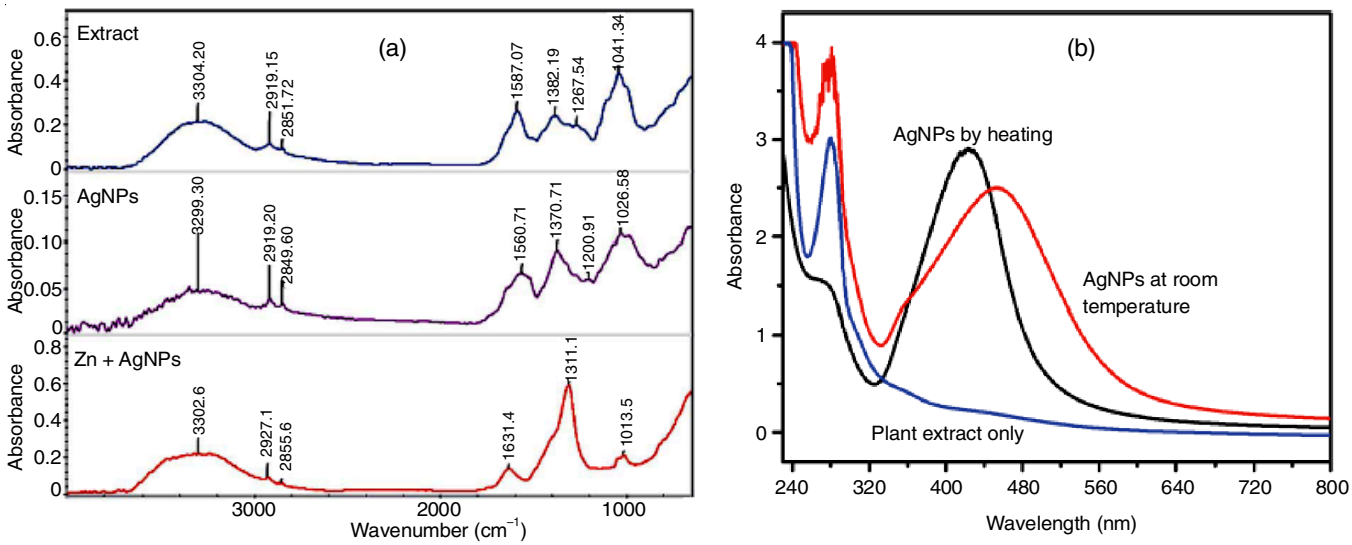

Fig. 4. (a) FTIR spectra of amomum subalatum extract, synthesized AgNPs and AgNPs presence in Zn^{2+} (b) UV-Vis absorption spectra of AgNPs adopted from Ihsan *et al.* [6]

reduced as Ag^+ ions and more than a suitable amount direct the secondary layer formation over the diminishment of electron density in a thin layer of AgNPs. The large absorption intensity increased at 3302 cm^{-1} in the IR spectrum shows the free form of hydroxyl (-OH) group in an extract from the AgNPs surface (Fig. 4b), which could be attributed to high stable AgNPs with maximum absorption intensity at 11. Both peak shift of plant extract and AgNPs says may occur structural changes compound of plant extract during AgNPs synthesis. The entirely vanish off SPR peak after 6 h reveals that Zn^{2+} does not move from stabilizing agent before completion of 6 h and it gives long term stability even after 9 months. Based on the result, it is suggested that strong binding Zn^{2+} ions moved away from the stabilizing agent on the surface of silver nanoparticles and it causes the decreased SPR intensity hence corresponding colour changes occurring on photographic images.

Niaz *et al.* [39] has demonstrated a similar kind of SPR peak disappearance in colorimetric detection of iodine ions over the synthesized tea-capped AgNPs using *Camellia sinensis* (green tea). In this study, a strong affinity of silver causes the disappearance of SPR from 405 nm. This mentioned that interaction ability of tea capped AgNPs with iodine ions and their diminishment of surface electrons of nanoparticles could be direct the decolorization of solution. The strong binding ability of iodine with Ag^0 produces the AgI formation through the absorption of iodine ions on the surface of AgNPs and their etching effect motivates decreased size of tea capped-AgNPs. The result obtained from TEM analysis, small size particles have appeared in the presence of iodine compared to the absence of iodine. However, the prepared AgNPs achieved a detection limit of 6.5×10^{-8} M with a linear range of 1×10^{-7} – 2.5×10^{-5} M [40]. Besides, detection of Pb^{2+} using AgNPs prepared from leaf extract of *Aconitum violaceum* and their catechol moiety structure in polyphenols compound used as colorimetric probes. The oxygen functionality of biomolecules could be used as a reducing and stabilization of AgNPs on the high basic medium of pH. The 1 mL of extract completely stabilized all Ag^+ ions while a higher amount of extract left in the solution causes the decreased absorption intensity in the SPR band. In this study, 6 h is required for the completion of AgNPs reduction to overcome the drawback of this reaction time reaction mixture heated above the 100 ºC for 5 min. The SPR peak is now showing become narrower from broadening at 404 nm. Hence, it is suggested that 5 min heating treatment completed a synthesis of AgNPs entirely instead of 6 h when using plant extract. They reported complex ability of Pb^{2+} reacted with electron donors of a hydroxyl group of catechins polyphenol on the surface of nanoparticles and it gives a Pb-catechins-AgNPs complexity formation, which is conformed from the exhibition of the new absorption peak at 520 nm in UV spectra. The corresponding absorption spectral changes indicate the concentration of Pb^{2+} is to act as a function of sensitivity [41]. In another interesting work, Li *et al.* [42] developed biologically functionalized CYs-AgNPs using *Citrullus lanatus* juice extract for the detection of nickel(II) ions. AgNPs surface modification over the –SH ligand group of L-cystein makes shifting of SPR peaks from 420 nm to 415 nm. The –COOH and $–NH_2$ groups in extract give a strong affinity with heavy metal ions and its surface provides stability of nanoparticles. While pH reaction and particle aggregation play an important key role in negatively charged binding sites of CYs. The desire surface functionality with different concentration nickel(II) ions gave the subsequent absorption changes in UV-vis spectra like 420 to 455 nm in CYs-AgNPs surface with nickel(II). Ain *et al.* [43] synthesized methyl gallate conjugated MG-AgNPs detection of gentamicin presence on interfering drugs and metal ions. They utilized nineteen commonly used drugs and medicines to evaluate their sensing capability. The carbonyl group of methyl gallate mainly contributes to the stabilization of MG-AgNPs. The proposed sensor fairly suitable for a wide range of pH like 4-10 with a detection limit of 0.29 µM because the hydroxyl group of gentamicin induces hydrogen bonding on methyl coated AgNPs. The resulted variation of UV-vis spectra reveals that aggregation, thermal stability (100 ºC) MG-AgNPs when the addition of gentamicin [44]. Singh *et al*. [45] pH trigged green AgNPs using epigallocatechin gallete for the detection of industrial useful kanamycin and environmentally hazardous sulfide ions. They checked detection ability by using different antibiotics because of the selectivity issues of AgNPs in an excess amount of other antibiotics. As from results; Ag^+ and quinone moieties generated on surfaces of AgNPs are subsequently reacted with multiple amounts of the amine group in kanamycin. The surface of AgNPs binds with kanamycin towards selective affinity exhibited with common antibiotics and observed radical decline. A noticeable change in SPR intensity band toward the longer wavelength appeared when the addition of kanamycin [45]. Also, the detection of sulfide ion's typical absorption peak exhibits distinct changes in their inter particle space. This result may due to the relation between the target molecule and AgNPs donor, acceptor or the formation of hydrogen bond. Similarly, Zheng *et al.* [46] used *Lycii fructus* synthesis of carbon dots functionalized CD-AgNPs for phoxim detection. They analyzed spectral changes from complex coordination of electrostatic interaction between positive charges of free amino and carboxylate groups in phoxim and negative charges of nitrogen containing ($-NH_2$), oxygen containing (-COOH) in carbon dots. Meanwhile, CDs-AgNPs aggregations are directed by the deprotonation of functional groups at alkaline conditions on the surface of carbon dots.

Electrochemical analysis of AgNPs: Over the past few years, many authors successfully investigated newly developed biosynthesis incorporated AgNPs approach for the detection of various metal ions and properties of the different electrode material through electrochemical techniques. The higher concentration of metal ions produces higher toxicity and can act as a serious threat to the neurodegenerative diseases on human beings [47]. Sophisticated facilities of the electrochemical method play a prominent role and though were inspired to great attention in the field of electrochemical sensors. Many sensors have been used as carrier electrochemical detection such as magnetic nanoparticles, metal nanoparticles, carbon nanotube and nanocluster, *etc*. [48]. Among the various metal nanoparticles by the nature of good electrical conductivity,

excellent electron transfer rates, low detection limits of silver nanoparticles are offered electrode surface modification [49]. However, the biosynthesized modified electrode having strong binding affinity, high surface to volume ratio, strong surface reaction and good absorption ability. Hence in this section need to discuss electrode sensing mechanism of ions encircling cyclic voltammetry (CV) and differential pulse voltammetry (DPV) approach are explained by some of following factors such as the effect of concentration, the effect of pH, the effect of scan rate, linear relationship, reproductively and selectivity of a modified electrode which are served as various ions detections.

Aravind *et al*. [3] shows an interesting unmodified AgNPs without surface functionalization using *Lycopersion esculentum* (LE) extract for electrochemical sensing of Cr(III) ions. The synthesized AgNPs SPR peak sharply obtained on 413 nm with a high extinction coefficient on pH 10 by the reason of mono-dispersed nature in a 1:4 ratio of leaf extract and $AgNO_3$. Various leaf extract ratio of 1:1,1:3 and lower than pH of 6 did not exhibit smooth SPR peak. Faster absorption observed on a short interval of time with high power irradiation, complete conversion of Ag^+ to Ag^0 within the 90 s is evidence that the formation of AgNPs affected by microwave irradiation time and power also. The citrate ion present on the surface of the AgNPs-LE changes the morphology of synthesized AgNPs-LE/Cr(III) complex from their spherical safe due to the aggregation and dense interaction of Cr(III) ions. Hence they can observe size variation from TEM images of AgNPs-LE/Cr(III) complex (18.31 nm) is larger than AgNPs-LE (10.82 nm) and peak diminishment occurred on XRD shows in Fig. 5. They performed AgNPs-LE-Pt electrode scanned with a potential range from -1 to +1 in a 0.15 M acetate buffer solution. The bare platinum electrode did not show the sensing response and found that AgNPs-LE with Cr(III) ions complex formation provides enhancement electron transport. In these findings, the redox peak gradually increases by the effect of concentration carried out ranges between 10 to 90 µm. The electrochemical reaction between AgNPs-LE and Cr(III) ions depends on the deposition of Cr(III) at the electrode surface and affected the accuracy of the reaction by their pH while changing from 6 to 13. They found to be enhanced redox peak current towards positive value when increasing scan rate from10 to100 mV s^{-1} by the irreversible system. This fact is employed to confirm of electron transfer reaction is a surface-confined one [50]. They were able to achieve high selectivity with a detection limit of 0.804 µm through the fabricated AgNPs-LE-Pt electrode sensor. Further, the same authors developed another one approach of highly sensitive detection on Cd(II) ions using AgNPs by *Allium sattivam* (AS) extract. In this work, they demonstrated the redox current response of the modified electrode of AgNPs-AS-Pt complex. The rich sulfur content in extract such as S-allyl cystein, S-allyl mercapto cystein, dialkyl trisulfide, dialkyl disulfide dialkyl sulfide is good to bind with Cd(II) ions, which are causes the size increment from 19.8 nm to 26.82 nm when interacting with the surface of AgNPs due to the aggregation on organosulfur complex formation. Intermolecular hydrogen bond formation while results on aggregation favourable detection of Cd(II) ions in the base medium of pH. The exhib-ition of linear increase of redox current response can be observed concerning the amount of concentration of Cd(II) ions, the creation of metal hydroxide influenced by the variation of pH and formation of AgNPs-AS-Pt complex. The mentioned factors make the accuracy of the sensing mechanism. Hence they concluded that AgNPs-AS-Pt modified electrode opt for selective sensing of Cd(II) ion with a lower detection limit of 0.227 µm [47]. Dodevska *et al.* [17] showed AgNPs reduction with four various (post distillation water, 30% ethanol, 70% ethanol) extract of *Rosa damascene* waste. The different extracts of *Rosa damascene* are induced some significant delay time in AgNPs formation and their effect making visual colour changes of the solution during the synthesis ex: 60 min for PW, 120 min for 30% EE, 360 min for 70% EE. The intensive absorption became unreadable after than 60 min due to the extent of nanoparticles agglomeration. The higher amount of catechin and epicatechein of polyphenols in 70% ethanolic extract and rich carbohydrates in PW extract could be used to achieving spherical nanoparticles with an average size of 25 nm, 11 nm respectively. The faster synthesis of AgNPs contains higher nanoparticle agglomeration. They have investigated the electrochemical performance of modified graphite electrode AgNPs/GE and chitosan electrode AgNPs/CS/GE recorded in a 0.2-0.8 V potential range of 25 mV s^{-1} scan rates. Their modification made on two different approaches of mechanical polishing: i) AgNPs/GE electrode prepared from 2 h absorption process of AgNPs colloidal solution at 25 ºC under in static condition; ii) AgNPs/CS/GE electrode prepared at room temperature through stabilization of electroactive layer with chitosan polymer film in air. Well defined pair of redox peak at 0.1 V indicating the existence of AgNPs at graphite surface and their shifting of peak potential from -0.4 V to positive direction exhibited catalytic activity of modified electrode towards H_2O_2 reduction. The two times higher amount of sensitivity to be found on AgNPs/GE electrode and significantly longer linear range of current response to be found on AgNPs/GS/GE electrode because of stabilizing effect of graphite surface through chitosan coating. Although they are discussed, amperometric quantitative tests for the detection of vanillin also, their steady-state current reached on within 20 s. The surface modifications of AgNPs/CS/GE electrode were able to detect up to a lower limit of 8.4 µm. Sebastian *et al.* [49] applied on a convenient approach of *Moringa oleifera* (MO) bark extract mediated AgNPs-MO. The rich benzyl glucosinolate in extract influences the AgNPs agglomeration and their sulfur group makes covalent bond formation with the surface of AgNPs. The aggregation of nanoparticles leads by the hydroxyl group of glucosinolate through the complex linkage of Cu(II)-O which causes the creation of a metal complex structure. They reported high selectivity of hazardous Cu ions detection in electrochemical redox performance. The sensing efficiency of developed AgNPs-MO/PE electrode with various metal ions exhibited sharp and clear redox peak due to the existence of AgNPs at the surface of the electrode and their characteristic features like porous structure, small size and large surface area could be increased the electrochemical response. Lokhande *et al.* [2] used to *Kimchi cabbage*

extract for the synthesis of AgNPs. The synthesized nanoparticles found to be on porous nature with an average size of 10-30 nm. The formed AgNPs obtained superior colloidal stability due to charge neutrality at AgNPs surface. Silver nanoparticles formation leads on by electron transfer to Ag^+ through the conversion process of flavonoid from enol to ketone due to the release of reactive hydrogen. The rapid nucleation occurs at Ag when their carboxyl group interacts with an electron in the $AgNO_3$ solution. They investigated the charge storage mechanism of Ag nanoparticles and elaborately studied their specific capacity, power density. The size variations and porous film structure existence of silver nanoparticles are enhanced by the supercapative mechanism. Moreover, electrochemical performance affected significantly by the provision of electro active surface area and their CV curve depicts the pseudo capacitive nature analyzed through strong redox peaks of AgNPs at 100 mV scan rate, voltage range from -1.2 to -0.5 V/SCE in 1 M NaOH. The magnitude of the oxidation-reduction current, clearly explain the conformation of electrooxidation and reduction transformation of AgO in electrode from the analysis of anodic and cathodic current at the end of each cycle, respectively. The complete oxidation of silver into AgO, AgO into Ag_2O could be attributed to achievable of fairly equal magnitude on the anodic and cathodic peak because of their one electron transformation reaction. The development of solid state structure is preferable for super active electrode material as well as it will be employed on energy storage applications.

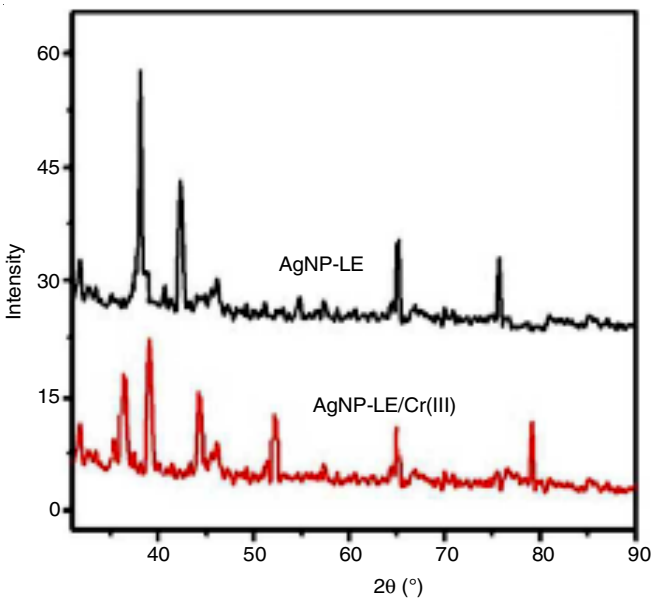

Fig. 5. XRD pattern of AgNPs-LE and AgNPs-LE/Cr(III) adopted from Aravind *et al.* [3]

Salazar *et al.* [51] prepared the silver nanoparticles-modified reduced graphene oxide nanocomposites (rGox/AgNPs) by tea extract carried out electrocatalytic properties of GCE/rGox/AgNPs electrode against the reduction of H_2O_2 detection in 0.1 M PBS. They displayed two well defined redox peaks at a particular range of potential in 0.05V and 0.4V and it to be shows reduction and oxidation of AgNPs found in GCE/rGox/AgNPs. This is ensuring that increase of the electro active surface of the sensor associated with the respective capacitive current. The intercalation of water molecules, oxide functional group formation causes the interlayer increases on the basal plane of carbon during chemical reduction with tea extract. When they realized high density plane edge of rGox defective sites are attributed notable reduction current by incorporation of graphene material and AgNPs electron transfer kinetic ascribed to graphene amplification opposite to H_2O_2 [52]. They suggested that kinetic boundaries are related to charge propagation on the characteristics of a non-controlled diffusion process and linear increase of both anodic, cathodic current against H_2O_2 with different scan rates. The selectivity of sensors tested in different biological interferences samples like dopamine, glutamate, glucose and ascorbic acid, respectively. They found to be highly reactive tea polyphenols allowing the reduction with water-soluble reducing agents. Shivakumar *et al.* [32] demonstrated the electrochemical sensing performance of AgNPs modified electrode using eucalyptus extract for the detection of nitrobenzene under the explored effect on pH. The microwave synthesized nanoparticles did not show the absorption variation after 10 min through the conversion of Ag^+ to Ag^0 completed within time. Negative charges in extract such as –OH and hemiacetal groups are attracted by AgNPs and it will restrict their size through the medium of a capping agent. The synthesized AgNPs/GCE exhibits higher reduction current peak and oxidation current peaks formed on subsequent anodic and cathodic current with a lesser potential of -0.816 V. AgNPs catalytic activity towards nitrobenzene evident from the formation of different species on an electrode and their change of the reduction current according to change of pH display the influence of proton concentration in reduction. This could be used for the detection of nitrobenzene existence in organic and inorganic compounds. In another study, AgNPs using *Talinum triangulare* (TT) demonstrate the faster charge transfer behaviour of TT-AgNPs/MWCNT modified electrode [18]. The synthesized TT-AgNPs were obtained nanoplate safe with rough surfaces due to extracting present on the surface of the particle, which is conformed from without definite safe of precursor morphology. The chelating ability of flavanoid is making a probability of interaction on aromatic ring nucleophilic character binding with metal. Even though it acts as an antioxidant, active oxygen scavenges process through donating the ability of electron or hydrogen atom. The extract contains proteins and enzymes could be facilitating pure metal AgNPs formation. Initially, they have observed an SPR peak at 418 nm after 90 min when continued reaction up to 20 h peak appeared at 430 nm. The reaction time shows the reduction of silver cations by the reason of the number of nanoparticles increasing. They found that pair of redox peaks by the attribution of AgNPs redox potential between MWCNT and TT-AgNPs due to ionic interaction. The electronic nature enhancing noticeable electron transport properties with CGE modification and their cloud nature gave a better performance in terms of oxidation potential, current recovery, stability and resistance of fouling effects, respectively. The irreversible diffusion controlled process used to higher Tafel value character to the absorption of reactants on the electrode surfaces. The modified electrode

stability tested from the storage in the refrigerator for some days, resulting in that no significant changes are observed. In the similar study, Kolya *et al.* [53] used *Mangifera indica* (MF) flower for the synthesis of AgNPs/rGO nanocomposites. The polyphenols present on the MF extract are attributed to the formation on spherical safe with AgNPs 8.5 nm due to Ag(I) ion reduction during on the synthesis and their carboxyl, epoxy and hydroxyl groups are making removal of oxygen functionality partially from rGO-$NaBH_4$-AgNPs. Hence, they obtained remarkable reduction efficiency causes by the decreases of interlayer distance at rGO-$NaBH_4$. The nature of rectangular shape cyclic voltammetry (CV) curve in different scan rates 10-200 mV s^{-1} in KOH shows the capacitive behaviour on without any significant redox peaks in conjugation extending at GO-Ag through π-π interaction. As well as found to be ionic fluxes at 10-30 mV s^{-1} scan rate and appeared distorted rectangular shape CV curve at higher scan rate. Fast moving ions in solution attributed decomposition of electrolyte and formation of electrical double layer. The specific capacitance drops at higher sweep rates because of ions are not fully diffuse into the inner active sites. The long term charge-discharge cyclic ability of specific capacitance was evidence that AgNPs/rGO utilized as an electrode material.

Catalytic applications of AgNPs: Recently, increasing dyeing and pigment industries are one of the major concerns problems of their non-biodegradable and toxic byproducts [54,55]. The waste effluents discharge from the array of industries such as leather, textile, plastic, paper, paint, cement, polymer, cosmetics and medicines and it is creating the severe environmental and human health problems by ungovernable dispenses in the atmosphere [56]. Naturally organic dyes are commonly used in catalytic degradation for removal of effluents even though it is a convenient treatment for the avoidance of toxic chemicals and significant human safety [57,58]. Hence in the existing scenario, necessary effort to develop ecofriendly, cost-effective, nontoxic methods for an answer to dye effluent pollution problem [59,60]. Silver based nanoparticles have been reported from ancient times to act as an efficient antimicrobial agent against bacteria and human pathogens [61]. This can enable them to degrade harmful organic dyes such as rhodamine B, methylene blue, methyl orange and Congo red [62]. The silver atoms are non-specifically oxidized as AgO_2 in the presence of oxygen and releasing Ag^+ ions in an aqueous medium. This can examine that silver is a powerful alternative oxidant agent for wastewater treatment technology [63]. The catalytic activity mechanism of AgNPs with mediated by various biological compounds. While the work of Nouri *et al.* [64] performed catalytic activity of *Mentha aquatic* leaf mediated AgNPs on methylene blue as a model dye. The oxidation of polyphenols in plant extract provides the free electrons to quinine for the reduction of Ag^+ ion into Ag^0 formation in alkaline conditions. The increasing pH of the colloidal solution causes the low level reduction ability of the extract and used to small size AgNPs formation. The different pH level indicates changes of affinity between AgNPs and methylene blue molecules and its causes to be decreased degradation rate. The amount of AgNPs leads to the enhanced increasing degradation rate exponentially. This result creates more amounts of sites and the availability of surfaces in catalytic reduction on methylene blue dye. While the electron transfers process facilitated by $NaBH_4$ attributes to the improved degradation rate of methylene blue in a limited period. Besides, they are evaluated catalytic reduction on various dyes like Congo red, rhodamine B and methyl orange with small of AgNPs and reported that green synthesized have more stability, more efficient, more reusability and low loss of AgNPs nanoparticles in wastewater treatment. Inspired by this work, Hamedi & Shojaosadati [65] reported that catalytic activity on AgNPs using *diospyros lotus* extract on the mixture of methylene blue and sodium borohydride. The synthesized AgNPs have defined border between nanoparticles with the size of 10-25 nm and did not change their absorption intensity after 30 min. This is insisted on the aggregation of the nanoparticles with suitable sustainability of capping agents in the plant extract. This ultimate stabilization is given by breakdown of H-bonds on the amide group in extract during on absorption of silver surfaces. The bond breaking energy creates the electron transfer facilities between methylene blue and $NaBH_4$ because it will act as a donor and acceptor respectively. Hence, AgNPs as an electron transfer mediator could accelerate the degradation rate of methylene blue dye in reduction and their maximum absorption band occurred at 664 nm due to the transition of π-π* and n-π*. Even though they experimented in a repeated manner for testing of recycling efficiency of AgNPs nanoparticles, do not observe the significant loss of catalytic activity. Similarly, Varadavenkatesan *et al.* [66] synthesized TGFE-AgNPs using *Thunbergia grandiflora* (TG) flower extract for catalytic study on degradation of Congo red dye. The large electrical charges in TG-SNP surfaces increased their stability by the reason of avoiding agglomeration. The optical density variation at maximum absorbance and their decolorization within 18 min are affirmed the Congo red dye reduction. The reduction-gum-degradation phenomenon of an azo group of dyes induced by the metal based nanoparticles and linear relationship from the normalized concentration-reaction time curve depicts their effectiveness, where TG-SNP acts as the electron transfer mediator during the reduction process. Nguyen *et al.* [19] *Stereospermum binhchauensis* and *Jasminum subtriplinerve* synthesized QBC-AgNPs, CV-AgNPs used for demonstration on catalytic degradation of organic contaminants like 4-nitrophenol, methyl orange using $NaBH_4$ in an aqueous medium. The UV-Vis spectral variation of synthesized QBC-AgNPs, CV-AgNPs exhibits morphology changes are induced by the organic compound present on the extract. The irregular shape QBC-AgNPs formed with a size range of 4-30 nm and consistent distribution of CV-AgNPs formed with a size range of 3-20 nm. This size distribution changes may explain from SEM images and reflects their effect of SPR peak as narrow or broader. The crystal orientation plane (111) is favoured for the growth of QBC-AgNPs, CV-AgNPs which is confirmed from obtained crystal lattice at 0.22 nm and 0.21 nm, respectively. Both synthesized AgNPs exothermic peaks have occurred above 300 ºC through the oxidation reactions. This indicates the metallic core of nanoparticles surrounded on biomolecules due to the

decomposition. The large redox potential difference between BH_4^- and 4-nitrophenol, methyl orange could be used to reduce the feasibility of reaction on kinetic barrier because of BH_4^- acts as an electron donor and 4-nitrophenol, methyl orange acts as an electron acceptor in the surface of metallic nanoparticles. The degradation evaluation 4-nitrophenol and methyl orange made on through the decreasing of absorption intensity in UV spectra and peaks of QBC-AgNPs, CV-AgNPs are reduced within 12, 6 min respectively. The consistent particle distribution and small size of CV-AgNPs lead to high catalytic activity and their fold degradation is 39-fold in 4-nitrophenol, as well as QBC-AgNPs, have 30 folds degradation. However, due to unfold high possibility of AgNPs can efficiently apply in industrial wastewater treatment [16]. Rashidi *et al*. [67] used to *Mespilus germanica* seed (MGS) for the synthesis of AgNPs/MGS nanophotocatalyst for efficiency evaluation of methylene blue dye in sunlight. The immobilization of AgNPs maintains the porosity structure without any agglomeration and small size nanoparticles formation by the ascorbic acid present in the surface of MGS extract. The nanophotocatalyst surface, active sites were affected by the variation of pH range from 6 to 10 and it will attribute the increasing degradation rate of methylene blue from 65% to 97%. This result indicates the importance of the utilization of sunlight as a free, endless, safe source. The interband transition of 4*d* to 5*sp* electrons interact with water-soluble oxygen molecule gives a formation of superoxide anion radicals (O^{2-}), redox reaction of resulting holes in silver reacted with water produce the hydroxyl cationic radicals ($OH^•$). Interestingly, this formed radical species (O_2^- and $OH^•$) degraded the methylene blue through the absorption of the catalytic surface. As expected, formed electron-hole pairs migrate to the surface of the catalyst as well as their higher energy states facilitate the increasing photodegradation due to the amount of photon absorbed from the sunlight. Kannan *et al.* [68] reported *Ludwigia octovalvis* leaf mediated AgNPs for photocatalytic activity against Alizarin red, Congo red, methylene blue and rhodamine B dyes. Undoubtedly, various hydroxyl groups presenting on the surface of AgNPs strongly interact with toxic dyes. This result suggested that photocatalytic dyes are degraded effectively through the breaking of electrons under sunlight irradiation.

Thatikayala *et al.* [69] used the *Tamarindus indica* pulp extract to synthesis of ZnO nanostructure covered AgNPs for photocatalytic activities of cationic and anionic dyes. The formation of Ag NSS sheets over on ZnO clearly explained the character of AgNPs in the redox peak recombination process and it will act as an electron sink through the making of oxygen molecules. The checking of dye stability in the presence of a catalyst in aqueous medium gives absorption and desorption phenomena are occurring in cationic dyes due to the negative charges in plant extract on the surface of ZnO/AgNPs. The Schottky barriers between ZnO and Ag lead to the Fermi level potential differences in the process of interfacial charge-transfer kinetics, recombination of electron-hole pair, which diminish the electron sink in Ag. Hence, the formation of superoxide anionic radicals (O^{2-}) and hydroxide radicals (-$OH^•$) with the reaction of oxygen molecules are approving the mineralization of pollutants of organic dyes and monomers possessing faster degradation rate. In a similar study, Rajith Kumar *et al.* [69] synthesized ZnO/AgNPs using *Calotropis gigantean* extract as a fuel in the combustion method for the photocatalytic activity of methylene blue degradation dye. The organic compound reaction gives a different morphology of nanoparticles like pyramidal, spherical and hexagonal safe with a diameter of 100-150 nm. The migration of charge carrier on catalyst surface generated superoxide and hydroxide radicals species are highly unstable during on reaction of organic compounds. They observed that the catalytic activity could be enhanced by size, safe, surface area, phase composition, bandgap and crystalline of ZnO/AgNPs. Shaikh *et al.* [20] synthesized AgNPs using *Shorea robusta* leaf extract for degradation of rhodamine B. The synthesized AgNPs stabilized on without aggregation at a higher concentration of extract due to the decreasing of particle size; this is observed from nature of SPR peak becoming narrow from broadening. In their work, they discussed some factors that are affecting the photocatalytic activity such as concentration, UV irradiation time, catalyst dose, pH and temperature. At low concentrations, rhodamine B dye were effectively degraded due to the production of $OH^•$ radicals and it will be accelerated in alkaline pH nature. However, charge carrier formation increased with increasing irradiation time as well as the rate of temperature plays a significant role in safe and size distributions. A notable amount of germination percentage during the photocatalytic process of rhodamine B explains the non-toxic nature of their byproducts. Nyabola *et al.* [70] used to *Aspilia plurisseta* extract synthesized AgNPs for catalytic activity against Congo red dye. The prepared spherical safe AgNPs with the size of 6 nm illustrate changes of morphology is influenced by the secondary metabolism of plant extracts like amides, acids and aliphatic amines. The SPR peak increased upto196 min of reaction time, which caused the size to change in nanoparticle formation. The degradation observed from the disappearance of naphthalene and benzene ring over the oxidation of N=N linkage fragmentation. The hydroxyl and oxygen radical formation directly tie-up with the photocatalytic action. Ravichandran *et al.* [71] demonstrated the photocatalytic activity of PAgNPs mediated by *Parkia speciosa* extract. The proteins, enzymes in extract could be stabilized the silver nanoparticles and their reduction of Ag^+ to Ag^0 made on through the releasing of the electron due to the breaking of O-H bond in flavanoid. The stable quinine obtained from the conversion of enol form in flavonoid. This case advocates that the electroactive nature of methylene blue dye could be accepting the electrons easily. Kadam *et al.* [72] synthesized AgNPs using cauliflower waste extract for degradation of phenol under sunlight. They investigate active species involvement in the catalytic reaction determined from triethanolamine (quencher of H^+) and nitrogen (quencher.O_2^-) over the trapping experiment and their absorption peak decreased from 270 nm indicates presents of AgNPs. Goswami *et al.* [73] achieved cellulose supported AgNPs supported from the extract of *Hibiscus sabdariffa* for the catalytic activity of the hazardous dyes. They studied the catalytic degradation of various organic dyes namely, methylene blue, methyl orange,

bromophenol blue, eosin Y and orange G. The AgNPs formation held by over the two process (i) electron rich functionality in extract combine with Ag^+ ions and (ii) formation of oligomeric clusters due to the hydroxyl group are presenting on nanocellulose. The uniform dispersion of silver nanoparticles shows that the activity of oxygen functional groups in cellulose through the immobilization of AgNPs. Importantly, silver atoms are an instrumental generation for the creation of free radicals possessing unpaired electrons and vacant *d*-orbital. The complex organic dye molecules carry on an increased rate of degradation through the transfer of an electron from the more number of active sites. In this context, the nanocellulose exposes the reactive hydroxyl group which is easily absorbed on the catalyst surface of the dye molecules. Lowest molecular weight and simplest structure dye molecules undergo fast degradation because of the resonance effect of N=N weakening by hydroxyl and amino functional groups. They found to be successful degradation for all dyes over the observation absorption peaks decreased gradually with exposure time. Besides, they suggested phenol ring in azo dyes to increase the rate of degradation at the position of *para* compound instead of substitution on *ortho*, *meta* compounds. Chandu *et al.* [74] reported the CRG-Ag nanocomposites using custard apple leaf for the photocatalytic activity of methylene blue dye as a model pollutant under the sunlight. The more number of C=C in CRG owing to enhance the conjugation through the π-π* and n-π* transition and oxygen functional group on GO removed by the reduction of Ag^+ ions with CLE extract. This reduction might be attributed without agglomeration of AgNPs with CRG sheets even though on high stability. The GO surface is act as a nucleation site by the attachment of a negatively charged oxygen functional group with Ag^+ ions like carboxyl and carbonyl group, which creates the diol-type moiety over the activation of protonation. Hence, AgNPs are well bound with GO surfaces despite the reduction of GO. The high surface areas of the graphene sheet with π-π interaction of aromatic regions promote the number of dye molecules adsorbed on GO surface. Especially, the degradation of methylene blue dye is generated photoelectrons through a redox reaction. The catalytic process increased by the mobility of conducting electrons as well as this study shows an improved degradation in limited time. Hence, could be used to water purification technology and dye sensitized solar cells. Some important photodegradation of biosynthesized AgNPs and their parameters are shown in Table-1.

Wound healing applications of AgNPs: Wound healing is a major part of the inflammatory process and can repair the injury to the skin and other soft tissues in human beings [75]. Wound infection is the most rigorous pain threshold in the period of surgical span and their very slow recovery creates the other problems of bacterial resistance, the occurrence of superbugs [76]. The bacteria colonization makes severe infections after infections such as cytotoxic wound microenvironment, delaying wound regeneration, causing much pain, distress and morbidity in patients sometimes may lead to disability, diseases and even in death also. To overcome these complications, we need ideal wound dressing material to have properties of biocompatible, biodegradable and moisture retentive. The incorporation of the mentioned character in one drug is often difficult and complex [77]. Hence, the development of simple wound bio drugs is still an inviting solution. Silver is a natural biomedical agent with wide applications in wound dressing management and plays a most effective role in bacterial infections. Green syntheses of modified silver nanoparticles with natural compounds can be utilized as effective dressing material in irregular wound compare than chemical method [78] and is used to promote the wound healing in some aspects such as non-toxic, non-allergenic, no-adherent to the skin, antibacterial capacity, possess adequate gas permeability, absorb excess exudates, maintain the wound surface with a moist environment, be removed with minimum pain [79].

Xuan *et al.* [78] used bFGF encapsulated CS-Ag hydrogel nanoparticles, which accelerated wound repair through the dual functionality of Ag^+ ions and the bFGF growth factor of fibroblast. The hydrogel SEM image depicts interconnected, loosely

TABLE-1
PHOTO DEGRADATION OF VARIOUS BIOSYNTHESIZED AgNPs

Catalyst	Pollutant dye	Source	Degradation time (min)	Degradation amount (%)	Applications	Ref.
CLW-AgNPs (cauliflower leaves)	Methylene blue	Sun light	150	90	–	[72]
ZnO/AgNSs (*Tamarindus indica* pulp)	Methylene blue, methyl orange	UV	120,150	98,81	Environmental issues	[68]
CRG-Ag (custard apple leaves)	Methylene blue	Sun light	30	96	DSSC	[74]
AgNPs (*Shorea robusta* leaves)	Rhodamine B	UV	90	90	–	[20]
AgNPs (*A. pluriseta* leaves)	Congo red	UV	30	50	Wastewater treatment, cosmetics	[70]
AgNPs/MGSNPC (*Mespilus germanica* seed)	Methylene blue	Sun light	35	97	–	[67]
ZnO/AgNPs (*Calotropis gigantea* leaves)	Methylene blue	UV	105	99	Wastewater treatment, medical applications	[79]
PagNPs (*Parkia speciosa* leaves)	Methylene blue	Sun light	180	84	Water purification, textiles industries	[71]
MAL-AgNPs (mentha aquatic leaves)	Methylene blue	UV	26	–	Wastewater treatment	[64]
QBC-AgNPs, CV-AgNPs (*Stereospemum binhchauensis*, jasmimum-subtriplinerve leaves)	4-Nitrophenol, methylene blue	UV	6,12	Completely	Industrial wastewater, environmental technology	[19]

packed microscopic pores bFGF@CS-Ag and their formation within 1 min and does not create any effect in the gelation process of CS-Ag. The bFGF@CS-Ag hydrogel showed a finer pro-healing effect, newly formed granulation tissue. This indicates the excellent antibacterial effect, antimicrobial functions of the CS-Ag group by the ability to release Ag^+ ions on bFGF, when the after-treatment of infected disease on the wound healing side. It is seen that wound exposure percentage of bFGF@CS-Ag hydrogel treated mice is smaller than other as well as brighter red blood vessels in the central wound region having the strongest fluorescence intensity. Notably, it shows the excellent regeneration of skin and successful growth factors of severe inflammation response on bacterial effect, which is served by oxygen and nutrients of newly formed blood vessels. Maghimaaa & Alharbib *et al.* [80] synthesized CL-AgNPs using *Curcuma longa* extract embedded in the cotton fabrics. The binding potential of the extract with AgNPs illustrates the best reduction in microbial growth through the amalgam formation of CL-AgNPs with cotton fabrics, which could be used to oxidize the molecular structure over the distribution of the Ag^+ ions due to the generation of oxygen radicals. They exhibited a noticeable wound healing potential of CL-AgNPs *via* increasing fibroblast proliferation and cell migration against the skin infection-causing pathogens even though their cell line did not possess any mild toxicity with treated synthesized nanoparticles because of oxygen diffuses on the surrounding medium from the fiber. The natural behaviour of cotton like softness, biodegradation, regeneration is may promote the wound healing contraction due to the binding capacity of nanoparticles. Recently, Ahsan & Farooq [81] synthesized AgNPs-Bc loading into PVA hydrogel using cabbage extract. The AgNP-hydrogel, AgNP-Bc-hydrogel network histopathological analysis exhibits excellent wound healing activity at regular intervals of time and their microporous and filamentous polymeric network structure of homogeneous distribution of AgNPs is favoured for oxygen passage on a wound. The presenting factor of gland cells, hair follicles, blood vessels, fibroblasts and a layer of the epidermis is indicated the epithelization completion in hematoxylin and eosin stained tissue through the inflammatory response even after 2 or 3 weeks disappearance of inflammatory cells. AgNPs-Bc-HP drugs are applied on the wound showed 0.30 ± 0.08 cm^2, which indicates better wound healing activities accelerated by AgNPs. Although, AgNPs with clay biocomposites are maximize the wound healing activity. The hydrogel polymer network releasing controllable AgNPs will keep the sterile environment around the wound. It is appreciated that avoiding scaling and dryness of wounds through their moisturizing properties. However, formed hydrogel mediating cellular apoptosis AgNPs with cabbage extract report that enhanced effect on cancer treatment, healing of chronic wounds and diabetic wounds. Tao *et al.* [23] synthesized AgNPs-sericin/PVA dressing for wound healing from the silkworm cocoon. The macroscopic structure with a pore size of 20-90 μM SP-Ag dressing is sufficient to demand of tissue generation because of normally pore size of 20-125 μM are able regeneration. The sericin/PVA interconnected structure not affected by the formation of AgNPs. They demonstrated desired high porosity, good wettability, hygroscopicity and mechanical property of hematoxylin and eosin. In particular, poor mechanical properties of sericin do not alter SP dressing tensile strength in softening of AgNPs and hydrophilicity, swelling properties are conserve the clammy environment through the penetrating of wound fluids. The reconstruction of venules and arterioles in control group SP-Ag specify revascularization and wound restoration over the recognized replacement of necrotic tissue by little collagen with neonatal fibroblast. Based on results, wound healing is promoted by collagen deposition and angiogenesis restoration capabilities of AgNPs are upgrade the wound healing activity. Very recently, Ravindran *et al.* [82] demonstrated wound healing effect of AgNPs from *Tridax procumbens* leaf extract. They made to attempt the dynamic process of regenerated superficial tissue and fish skin healing. In this context, the initial period of injury makes cellular changes of epithelial layers on target organs and it exhibited a partial loss of stratified squamous cell layer. They observed hemorrhage formation and collagen deposition on the skin surface due to the *Tridax procumbens* leaf extract healing effect. The control group depicts the formation of infiltration of inflammatory cells, necrosis of epidermis and dermis due to damage of blood vessels. The identical re-epithelialization appeared on both such as fish and human skin. Wang *et al.* [83] demonstrated the biofabrication of AgNPs synthesis from *Deloix eleta* leaf extract could be used as an effective wound healing agent. In this study, wound area closure observed by the daily repeated basics in terms of the degree of percentage appeared on the nm scale. They were observed drastic changes of wound contraction from 11.32 to 0.02 mm on muslin cloth coated AgNPs on after 17 days. Meanwhile, this is happened by AgNPs capability to make changes in the immunomodulation, cytok modulation of the wound. Wang *et al.* [84] synthesized CS-OKGM/AgNPs hydrogel for the wound healing process. The prepared AgNPs was to be found in the size of 9 nm in OKGM solution, which is favourably accelerating the gellation mixture over the easy reaction of the amino group in chitosan with an aldehyde of OKGM as well as the Schiff-base reaction between an amino group in tissue protein and aldehyde in hydrogel gives a satisfactory adhesive performance of the gel. Hence tissue osmotic fluid absorbed on the wound site and their surface adhered tightly. The higher amount of aldehyde group leads to short gellation time (10 s), this could be used to quickly fill up the entire defect surface. The hydrogel of CS-OKGM/AgNPs shows overheating of wound surface making a relive from wound infections and it appeared as like as normal skin temperature. This is evidence from the infrared thermal images of wound in Fig. 6. The designed CS-OKGM/AgNPs exhibited unparalleled wound self-healing ability, effective re-epithelization and fibroblasts tissue remodeling arrangement. At last, Tong *et al*. [85] used DNA-guided silver nanoparticles on graphene oxide to evaluate the wound healing capability through the morphological difference in mice tissue. The interaction of Ag^+ with an oxygen-containing group of ssDNA making an attachment of AgNPs to GO surface, which could be attributed coverage of AgNPs uniformly on the surface of the GO and their contribution causes the spherical like AgNPs,

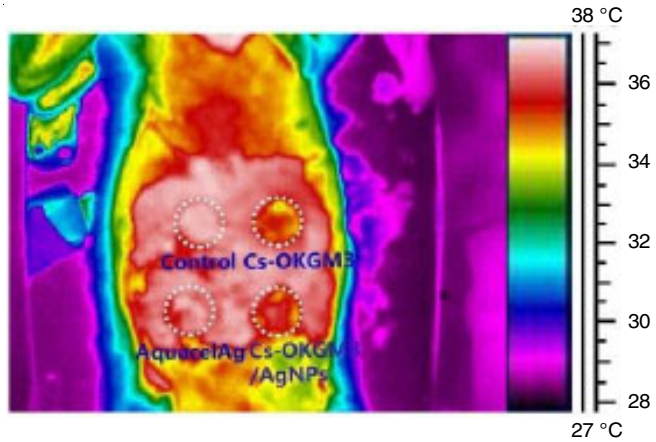

Fig. 6. Infrared thermal image of wound adopted from Wang *et al.* [84]

stable sheet structure GO with good transparency. The elongated fibroblasts and epithelial cells in wound dressing migrate the re-epithelization signals and it is useful for the formation of granulation tissues, which contained on the ssDNA-AgNPs@GO treatment group. The ssDNA-AgNPs or GO treatment group obtained many lymphocyte and neutrophil cells are reflecting the inflammatory response opposite to the ssDNA-AgNPs@GO treatment group. Thus, the results reported the re-epithelialization and dense collagen deposition properties were build-up the wound healing.

Conclusion

In this review, various biocompound functionalization utilized on the biomass derivable silver nanoparticles synthesis are summarized. Most of them are listed here based on the consideration of human health and environmental issues. Rightly, choosing a different type of bio-functionalization process used to make suitable properties for various applications of silver nanoparticles. Bioextract mediated nanoparticle fabrication approach is human friendly and phyto-accumulation in plants significantly enhances the uptake of silver without any toxicants, contribute as reduction as well as the stabilizing agent. Green production of silver nanoparticles having lower possible risk in wound regeneration due to their lower cytotoxic mechanism and well adaptation of biotemplates offer the antimicrobial resistance to antibiotics. Hence, can be utilized it as a successful drug for treating a wound. According to different researchers' opinions on the proposed mechanism of photodegradation, active radicals like hydroxyl ($^{\bullet}OH$), hydroperoxyl ($HO_2^{\bullet}$) and superoxide ($O_2^{\bullet-}$) perform a predominant role in the catalytic process. Phytochemicals loading are attributed charge separation on silver nanoparticles, which is highly useful in the bioremediation of industrial wastewater. The developed electrode exhibits better integration of biological compound with AgNPs and its present are giving to an understanding of electroanalytical sensing of trace level detection of metal ions and long term stability of energy storage material. Finally, the surface plasmon resonance (SPR) effect is an effective nano-weapon for the detection of optical emission detection, the AgNPs modification of biological molecules is the ability to use multi-target practical applications of chemical and biosensors. Hence will be continued to expand the bio-synthesized silver nanoparticles to solve and recover from the environmental problems in the near and future.

ACKNOWLEDGEMENTS

This work is financially suppored by Kalasalingam Academy of Research and Education.

CONFLICT OF INTEREST

The authors declare that there is no conflict of interests regarding the publication of this article.

REFERENCES

1. N. Sultana, P.K. Raul, D. Goswami, D. Das, S. Islam, V. Tyagi, B. Das, H.K. Gogoi, P. Chattopadhyay and P.S. Raju, *RSC Adv.*, **10**, 9356 (2020); https://doi.org/10.1039/C9RA09972G
2. A.C. Lokhande, P.T. Babar, V.C. Karade, J.S. Jang, V.C. Lokhande, D.J. Lee, I.-C. Kim, S.P. Patole, I.A. Qattan, C.D. Lokhande and J.H. Kim, *Mater. Today Chem.*, **14**, 100181 (2019); https://doi.org/10.1016/j.mtchem.2019.07.003
3. A. Aravind, M. Sebastian and B. Mathew, *Environ. Sci. Water Res. Technol.*, **4**, 1531 (2018); https://doi.org/10.1039/C8EW00374B
4. A. Abdolmaleki, A. Asadi, K. Gurushankar, T.K. Shayan and F.A. Sarvestani, *Adv. Pharm. Bull.*, **11**, 450 (2021) https://doi.org/10.34172/apb.2021.052
5. J. Hsiao, S. Chen, B. Hung, K. Uma, W. Chen, C. Kuo and J. Lin, *RSC Adv.*, **10**, 7551 (2020); https://doi.org/10.1039/C9RA10462C
6. M. Ihsan, A. Niaz, A. Rahim, M. Zaman, M. Arain, T. Sirajuddin, T. Sharif and M. Najeeb, *RSC Adv.*, **5**, 91158 (2015); https://doi.org/10.1039/C5RA17055A
7. K. Mijnendonckx, M.M. Ali, A. Provoost, P. Janssen, M. Mergeay, N. Leys, D. Charlier, P. Monsieurs and R. Van Houdt, *Metallomics*, **11**, 1912 (2019); https://doi.org/10.1039/C9MT00123A
8. A.A. Hamed, H. Kabary, M. Khedr and A.N. Emam, *RSC Adv.*, **10**, 10361 (2020); https://doi.org/10.1039/C9RA11021F
9. Y. Pan, W.J. Paschoalino, S.S. Bayram, A.S. Blum and J. Mauzeroll, *Nanoscale*, **11**, 18595 (2019); https://doi.org/10.1039/C9NR04464G
10. L. Sethuram, J. Thomas, A. Mukherjee and N. Chandrasekaran, *RSC Adv.*, **9**, 35677 (2019); https://doi.org/10.1039/C9RA06913E
11. H. Li, J. Chen, H. Fan, R. Cai, X. Gao, D. Meng, Y. Ji, C. Chen, L. Wang and X. Wu, *Nanoscale*, **12**, 6429 (2020); https://doi.org/10.1039/C9NR08621H
12. M. Wang, W. Zhang, X. Zheng and P. Zhu, *RSC Adv.*, **7**, 12144 (2017); https://doi.org/10.1039/C6RA27706C
13. D. Kumar, M. Nair and R. Painuli, *Plasmonics*, **14**, 303 (2019); https://doi.org/10.1007/s11468-018-0805-4
14. B. Vellaichamy and P. Periakaruppan, *RSC Adv.*, **6**, 35778 (2016); https://doi.org/10.1039/C6RA04381J
15. R.A. Dar, N.G. Khare, D.P. Cole, S.P. Karna and A.K. Srivastava, *RSC Adv.*, **4**, 14432 (2014); https://doi.org/10.1039/C4RA00934G
16. K. Nitinaivinij, T. Parnklang, C. Thammacharoen, S. Ekgasit and K. Wongravee, *Anal. Methods*, **6**, 9816 (2014); https://doi.org/10.1039/C4AY02339K
17. T. Dodevska, I. Vasileva, P. Denev, D. Karashanova, B. Georgieva, D. Kovacheva, N. Yantcheva and A. Slavov, *Mater. Chem. Phys.*, **231**, 335 (2019); https://doi.org/10.1016/j.matchemphys.2019.04.030
18. E.E. Elemike, D.C. Onwudiwe, O.E. Fayemi, A.C. Ekennia, E.E. Ebenso and L.R. Tiedt, *J. Cluster Sci.*, **28**, 309 (2017); https://doi.org/10.1007/s10876-016-1087-7

19. T.M.-T. Nguyen, T.T.-T. Huynh, C.-H. Dang, D.-T. Mai, T.T.-N. Nguyen, D.-T. Nguyen, V.-S. Dang, T.-D. Nguyen and T.-D. Nguyen, *Res. Chem. Intermed.*, **46**, 1975 (2020); https://doi.org/10.1007/s11164-019-04075-w
20. W.A. Shaikh, S. Chakraborty and R.U. Islam, *Int. J. Environ. Sci. Technol.*, **17**, 2059 (2020); https://doi.org/10.1007/s13762-019-02473-6
21. D. Sarathi Kannan, S. Mahboob, K.A. Al-Ghanim and P. Venkatachalam, *J. Cluster Sci.*, **32**, 255 (2020); https://doi.org/10.1007/s10876-020-01784-w
22. A. Chandra and M. Singh, *Inorg. Chem. Front.*, **5**, 233 (2018); https://doi.org/10.1039/C7QI00569E
23. G. Tao, R. Cai, Y. Wang, L. Liu, H. Zuo, P. Zhao, A. Umar, C. Mao, Q. Xia and H. He, *Mater. Des.*, **180**, 107940 (2019); https://doi.org/10.1016/j.matdes.2019.107940
24. M. Zhang, Y.-Q. Liu and B.-C. Ye, *Analyst*, **137**, 601 (2012); https://doi.org/10.1039/C1AN15909G
25. D. Dai, Z. Li, J. Yang, C. Wang, J.-R. Wu, Y. Wang, D. Zhang and Y.-W. Yang, *J. Am. Chem. Soc.*, **141**, 4756 (2019); https://doi.org/10.1021/jacs.9b01546
26. C. Burda, X. Chen, R. Narayanan and M.A. El-Sayed, *Chem. Rev.*, **105**, 1025 (2005); https://doi.org/10.1021/cr030063a
27. Y. Leng, K. Xie, L. Ye, G. Li, Z. Lu and J. He, *Talanta*, **139**, 89 (2015); https://doi.org/10.1016/j.talanta.2015.02.038
28. M.R. Bindhu and M. Umadevi, *Spectrochim. Acta A Mol. Biomol. Spectrosc.*, **121**, 596 (2014); https://doi.org/10.1016/j.saa.2013.11.019
29. S. Das, M.N. Aktara, N.K. Sahoo, P.K. Jha and M. Hossain, *J. Environ. Chem. Eng.*, **5**, 5645 (2017); https://doi.org/10.1016/j.jece.2017.10.053
30. Y. Wang and Y. Xia, *Mikrochim. Acta*, **186**, 50 (2019); https://doi.org/10.1007/s00604-018-3110-1
31. J. Hai, F. Chen, J. Su, F. Xu and B. Wang, *Anal. Chem.*, **90**, 4909 (2018); https://doi.org/10.1021/acs.analchem.8b00710
32. M. Shivakumar, M.S. Dharmaprakash, S. Manjappa and K.L. Nagashree, *J. Iran. Chem. Soc.*, **17**, 893 (2020); https://doi.org/10.1007/s13738-019-01822-z
33. P. Jarujamrus, M. Amatatongchai, A. Thima, T. Khongrangdee and C. Mongkontong, *Spectrochim. Acta A Mol. Biomol. Spectrosc.*, **142**, 86 (2015); https://doi.org/10.1016/j.saa.2015.01.084
34. F. Samari, H. Salehipoor, E. Eftekhar and S. Yousefinejad, *New J. Chem.*, **42**, 15905 (2018); https://doi.org/10.1039/C8NJ03156H
35. M. Annadhasan, T. Muthukumarasamyvel, V.R. Sankar Babu and N. Rajendiran, *ACS Sustain. Chem.& Eng.*, **2**, 887 (2014); https://doi.org/10.1021/sc400500z
36. B. Vellaichamy and P. Periakaruppan, *New J. Chem.*, **41**, 4006 (2017); https://doi.org/10.1039/C7NJ00084G
37. V.N. Mehta, J.V. Rohit and S.K. Kailasa, *New J. Chem.*, **40**, 4566 (2016); https://doi.org/10.1039/C5NJ03454J
38. S. Jabariyan and M.A. Zanjanchi, *Appl. Phys., A Mater. Sci. Process.*, **125**, 872 (2019); https://doi.org/10.1007/s00339-019-3167-7
39. A. Niaz, A. Bibi, M.I. Huma, M.I. Zaman, M. Khan and A. Rahim, *J. Mol. Liq.*, **249**, 1047 (2018); https://doi.org/10.1016/j.molliq.2017.11.151
40. Y. Ling, Z.F. Gao, Q. Zhou, N.B. Li and H.Q. Luo, *Anal. Chem.*, **87**, 1575 (2015); https://doi.org/10.1021/ac504023b
41. K. Farhadi, M. Forough, R. Molaei, S. Hajizadeh and A. Rafipour, *Sens. Actuators B Chem.*, **161**, 880 (2012); https://doi.org/10.1016/j.snb.2011.11.052
42. H. Li, Z. Cui and C. Han, *Sens. Actuators B Chem.*, **143**, 87 (2009); https://doi.org/10.1016/j.snb.2009.09.013
43. N. ul Ain, Z. Aslam, M. Yousuf, W.A. Waseem, S. Bano, I. Anis, F. Ahmed, S. Faizi, M. I. Malik and M. R. Shah, *New J. Chem.*, **43**, 1972 (2019); https://doi.org/10.1039/C8NJ04565H
44. F.L. Palhano, J. Lee, N.P. Grimster and J.W. Kelly, *J. Am. Chem. Soc.*, **135**, 7503 (2013); https://doi.org/10.1021/ja3115696
45. R.K. Singh, B. Panigrahi, S. Mishra, B. Das, R. Jayabalan, P.K. Parhi and D. Mandal, *J. Mol. Liq.*, **269**, 269 (2018); https://doi.org/10.1016/j.molliq.2018.08.056
46. M. Zheng, C. Wang, Y. Wang, W. Wei, S. Ma, X. Sun and J. He, *Talanta*, **185**, 309 (2018); https://doi.org/10.1016/j.talanta.2018.03.066
47. A. Aravind, M. Sebastian and B. Mathew, *New J. Chem.*, **42**, 15022 (2018); https://doi.org/10.1039/C8NJ03696A
48. S. Senthilkumar and R. Saraswathi, *Sens. Actuators B Chem.*, **141**, 65 (2009); https://doi.org/10.1016/j.snb.2009.05.029
49. M. Sebastian, A. Aravind and B. Mathew, *BioNanoSci.*, **9**, 373 (2019); https://doi.org/10.1007/s12668-019-0608-x
50. L. Wang, H. Zhu, H. Hou, Z. Zhang, X. Xiao and Y. Song, *J. Solid State Electrochem.*, **16**, 1693 (2012); https://doi.org/10.1007/s10008-011-1576-4
51. P. Salazar, I. Fernández, M.C. Rodríguez, A. Hernández-Creus and J.L. González-Mora, *J. Electroanal. Chem.*, **855**, 113638 (2019); https://doi.org/10.1016/j.jelechem.2019.113638
52. N. Abdul Halim, Y. Lee, R. Marugan and U. Hashim, *Biosensors*, **7**, 38 (2017); https://doi.org/10.3390/bios7030038
53. H. Kolya, T. Kuila, N.H. Kim and J.H. Lee, *Compos. B. Eng.*, **173**, 106924 (2019); https://doi.org/10.1016/j.compositesb.2019.106924
54. S. Abdpour, E. Kowsari, M.R. Alavi Moghaddam, L. Schmolke and C. Janiak, *J. Solid State Chem.*, **266**, 54 (2018); https://doi.org/10.1016/j.jssc.2018.07.006
55. M.A. Mohd Adnan, N. Muhd Julkapli, M.N.I. Amir and A. Maamor, *Int. J. Environ. Sci. Technol.*, **16**, 547 (2019); https://doi.org/10.1007/s13762-018-1857-x
56. T.N.J.I. Edison, R. Atchudan, M.G. Sethuraman and Y.R. Lee, *J. Photochem. Photobiol. B*, **162**, 604 (2016); https://doi.org/10.1016/j.jphotobiol.2016.07.040
57. M. Khatami, R.S. Varma, N. Zafarnia, H. Yaghoobi, M. Sarani and V.G. Kumar, *Sustain. Chem. Pharm.*, **10**, 9 (2018); https://doi.org/10.1016/j.scp.2018.08.001
58. N. Wang, Y. Hu and Z. Zhang, *Appl. Clay Sci.*, **150**, 47 (2017); https://doi.org/10.1016/j.clay.2017.08.024
59. B.N. Patil and T.C. Taranath, *Microb. Pathog.*, **115**, 227 (2018); https://doi.org/10.1016/j.micpath.2017.12.035
60. A. Desireddy, B.E. Conn, J. Guo, B. Yoon, R.N. Barnett, B.M. Monahan, K. Kirschbaum, W.P. Griffith, R.L. Whetten, U. Landman and T.P. Bigioni, *Nature*, **501**, 399 (2013); https://doi.org/10.1038/nature12523
61. J. Saha, A. Begum, A. Mukherjee and S. Kumar, *Sustain. Environ. Res.*, **27**, 245 (2017); https://doi.org/10.1016/j.serj.2017.04.003
62. K.O. Shittu and O. Ihebunna, *Adv. Nat. Sci. Nanosci. Nanotechnol.*, **8**, 045003 (2017); https://doi.org/10.1088/2043-6254/aa8536
63. Y.-Y. Lau, Y.-S. Wong, T.-T. Teng, N. Morad, M. Rafatullah and S.-A. Ong, *RSC Adv.*, **5**, 34206 (2015); https://doi.org/10.1039/C5RA01346A
64. A. Nouri, M. Tavakkoli Yaraki, A. Lajevardi, Z. Rezaei, M. Ghorbanpour and M. Tanzifi, *J. Colloid Interface Sci.*, **35**, 100252 (2020); https://doi.org/10.1016/j.colcom.2020.100252
65. S. Hamedi and S.A. Shojaosadati, *Polyhedron*, **171**, 172 (2019); https://doi.org/10.1016/j.poly.2019.07.010
66. T. Varadavenkatesan, R. Selvaraj and R. Vinayagam, *Mater. Today*, **23**, 27 (2020); https://doi.org/10.1016/j.matpr.2019.04.216
67. M. Rashidi, M.R. Islami and D. Tahmassebi, *SN Appl. Sci.*, **2**, 668 (2020); https://doi.org/10.1007/s42452-020-2471-3
68. D. Thatikayala, V. Banothu, J. Kim, D.S. Shin, S. Vijayalakshmi and J. Park, *J. Mater. Sci. Mater. Electron.*, **31**, 5324 (2020); https://doi.org/10.1007/s10854-020-03093-4

69. C.R. Rajith Kumar, V.S. Betageri, G. Nagaraju, G.H. Pujar, H.S. Onkarappa and M.S. Latha, *J. Inorg. Organomet. Polym.*, **30**, 3410 (2020); https://doi.org/10.1007/s10904-020-01507-8
70. A.O. Nyabola, P.G. Kareru, E.S. Madivoli, S.I. Wanakai and E.G. Maina, *J. Inorg. Organomet. Polym.*, **30**, 3493 (2020); https://doi.org/10.1007/s10904-020-01497-7
71. V. Ravichandran, S. Vasanthi, S. Shalini, S.A.A. Shah, M. Tripathy and N. Paliwal, *Results Phys.*, **15**, 102565 (2019); https://doi.org/10.1016/j.rinp.2019.102565
72. J. Kadam, P. Dhawal, S. Barve and S. Kakodkar, *SN Appl. Sci.*, **2**, 738 (2020); https://doi.org/10.1007/s42452-020-2543-4
73. M. Goswami, D. Baruah and A.M. Das, *New J. Chem.*, **42**, 10868 (2018); https://doi.org/10.1039/C8NJ00526E
74. B. Chandu, C.M. Kurmarayuni, S. Kurapati and H.B. Bollikolla, *Carbon Lett.*, **30**, 225 (2020); https://doi.org/10.1007/s42823-019-00091-3
75. A. Gupta, S.M. Briffa, S. Swingler, H. Gibson, V. Kannappan, G. Adamus, M. Kowalczuk, C. Martin and I. Radecka, *Biomacromolecules*, **21**, 1802 (2020); https://doi.org/10.1021/acs.biomac.9b01724
76. Q. Zhang, C.-Y. Shi, D.-H. Qu, Y.-T. Long, B.L. Feringa and H. Tian, *Sci. Adv.*, **4**, 7 (2018); https://doi.org/10.1126/sciadv.aat8192
77. R. Manikandan, R. Anjali, M. Beulaja, N.M. Prabhu, A. Koodalingam, G. Saiprasad, P. Chitra and M. Arumugam, *Process Biochem.*, **79**, 135 (2019); https://doi.org/10.1016/j.procbio.2019.01.013
78. X. Xuan, Y. Zhou, A. Chen, S. Zheng, Y. An, H. He, W. Huang, Y. Chen, Y. Yang, S. Li, T. Xuan, J. Xiao, X. Li and J. Wu, *J. Mater. Chem. B Mater. Biol. Med.*, **8**, 1359 (2020); https://doi.org/10.1039/C9TB02331C
79. F. Paladini and M. Pollini, *Materials*, **12**, 2540 (2019); https://doi.org/10.3390/ma12162540
80. M. Maghimaa and S.A. Alharbi, *J. Photochem. Photobiol.*, **204**, 111806 (2020); https://doi.org/10.1016/j.jphotobiol.2020.111806
81. A. Ahsan and M.A. Farooq, *J. Drug Deliv. Sci. Technol.*, **54**, 101308 (2019); https://doi.org/10.1016/j.jddst.2019.101308
82. J. Ravindran, V. Arumugasamy and A. Baskaran, *Wound Med.*, **27**, 100170 (2019); https://doi.org/10.1016/j.wndm.2019.100170
83. S.-M. Wang, M.-L. Yu, K. Feng, X.-B. Li, Y.-Z. Chen, B. Chen, C.-H. Tung and L.-Z. Wu, *J. Photochem. Photobiol.*, **355**, 457 (2018); https://doi.org/10.1016/j.jphotochem.2017.06.038
84. Y. Wang, R. Xie, Q. Li, F. Dai, G. Lan, S. Shang and F. Lu, *Biomater. Sci.*, **8**, 1910 (2020); https://doi.org/10.1039/C9BM01635J
85. C. Tong, W. Zou, W. Ning, J. Fan, L. Li, B. Liu and X. Liu, *RSC Adv.*, **8**, 28238 (2018); https://doi.org/10.1039/C8RA04933E